Oncogene (2012) 1–11

www.nature.com/Oncogene

ORIGINAL ARTICLE

ETV5 cooperates with LPP as a sensor of extracellular signals and promotes EMT in endometrial carcinomas

E Colas[1,9], L Muinelo-Romay[2], L Alonso-Alconada[2], M Llaurado[1], M Monge[1], J Barbazan[2], M Gonzalez[1], M Schoumacher[3], N Pedrola[1], T Ertekin[1], L Devis[1], A Ruiz[1], J Castellvi[4], A Doll[1], A Gil-Moreno[5,9], M Vazquez-Levin[6], L Lapyckyj[6], R Lopez-Lopez[2], S Robine[3], E Friederich[7], M Castro[8], J Reventos[1,9], D Vignjevic[3] and M Abal[1,2]

Endometrial carcinoma (EC) is the most frequent among infiltrating tumors of the female genital tract, with myometrial invasion representing an increase in the rate of recurrences and a decrease in survival. We have previously described ETV5 transcription factor associated with myometrial infiltration in human ECs. In this work, we further investigated ETV5 orchestrating downstream effects to confer the tumor the invasive capabilities needed to disseminate in the early stages of EC dissemination. Molecular profiling evidenced ETV5 having a direct role on epithelial-to-mesenchymal transition (EMT). In particular, ETV5 modulated Zeb1 expression and E-Cadherin repression leading to a complete reorganization of cell–cell and cell–substrate contacts. ETV5-promoted EMT resulted in the acquisition of migratory and invasive capabilities in endometrial cell lines. Furthermore, we identified the lipoma-preferred partner protein as a regulatory partner of ETV5, acting as a sensor for extracellular signals promoting tumor invasion. All together, we propose ETV5-transcriptional regulation of the EMT process through a crosstalk with the tumor surrounding microenvironment, as a principal event initiating EC invasion.

Oncogene advance online publication, 23 January 2012; doi:10.1038/onc.2011.632

Keywords: ETV5; EMT; LPP; carcinoma invasion; endometrial cancer

INTRODUCTION

Endometrial carcinoma (EC), the most frequently diagnosed malignancy of the female genital tract in industrialized countries, is associated with a relatively low mortality.[1] Unfortunately, at the time of diagnosis, 20% of the patients present myometrial invasion and/or lymph node affectation, which are main indicators of an advanced disease, related to poor prognosis and decrease in survival rate. In particular, myometrial invasion represents at the clinical level an increase in the rate of recurrence after a first surgical treatment and a decrease in survival at the 5-year follow-up. Despite the characterization of molecular events associated with the development of EC, the molecular pathology of myometrial infiltration that defines the initial steps of invasion in endometrial cancer remains poorly understood.[2]

The epithelial-to-mesenchymal transition (EMT) has been pointed out as a crucial process in tumor invasion, whereby cells lose epithelial polarity and cell–cell contacts to acquire mesenchymal properties. Several recent reviews have summarized key signaling pathways involved in EMT and probed the link between the tumor microenvironment, EMT and cancer progression.[3–5] Hence, transformed cancer cells might be able to detach, penetrate through the basement membrane and infiltrate surrounding tissues to thereafter metastasize to secondary sites [6,7] by establishing complex interactions with its microenvironment.[8,9] To date, most of the signals inducing EMT exert their action through the modulation of transcription factors that repress epithelial genes, such as those encoding E-cadherin and cytokeratins.[4,10] Specifically, loss of E-cadherin has been described as the hallmark of EMT, and its transcriptional regulation through snail-related zinc finger factors, which directly binds to the E-boxes of E-cadherin promoter region, has been broadly studied to understand this phenomenon.[11–14] In addition to tumor cells infiltrating the myometrium, carcinoma invasion also involve the reactive stroma interacting with the tumor, the inflammatory components activated in reaction to the act of invasion and the activated endothelial cells associated with angiogenesis. All these components have essential roles in the initial steps of infiltration and dissemination.[15,16] Revealing the molecular pathways towards advanced tumorigenesis in EC, such as the control of the EMT process and the crosstalk between the tumor and its microenvironment, would be beneficial to increase our knowledge on the causes, which determine invasion.

We have previously characterized the upregulation of the *ETV5* gene in EEC, with a specific and significant increase restricted to those tumor stages associated with myometrial infiltration.[17,18] ETV5 belongs to the PEA3 subfamily of Ets transcription factors, characterized by a sequence of ~85 amino acids in an evolutionarily conserved DNA-binding domain that regulates the expression of a variety of genes by binding to a central A/GGAA/T core motif, in cooperation with other transcriptional factors and

[1]Biomedical Research Unit, Research Institute Vall d'Hebron University Hospital, Barcelona, Spain; [2]Translational Laboratory/Medical Oncology Department, Complexo Hospitalario Universitario de Santiago/SERGAS, Santiago de Compostela, Spain; [3]UMR 144 Centre National de la Recherche Scientifique, Institut Curie, Paris, France; [4]Department of Gynecological Oncology, Vall d'Hebron University Hospital, Barcelona, Spain; [5]Department of Pathology, Vall d'Hebron University Hospital, Barcelona, Spain; [6]Instituto de Biologia y Medicina Experimental, National Research Council of Argentina (CONICET), Buenos Aires, Argentina; [7]Life Science Research Unit, University of Luxembourg, Luxembourg, Luxembourg; [8]BioFarma Research Group, Department of Pharmacology, University of Santiago de Compostela, Santiago de Compostela, Spain and [9]Universitat Autonoma de Barcelona, Barcelona, Spain. Correspondence: Dr M Abal, Translational Laboratory/Medical Oncology Department, Complexo Hospitalario Universitario de Santiago/SERGAS; Trav. Choupana s/n Santiago de Compostela 15706, Spain. E-mail: miguel.abal.posada@sergas.es
Received 8 August 2011; revised and accepted 28 November 2011

cofactors.[19,20] Activation of MMP2 underlies the involvement of ETV5 in EC invasion.[21] In the present study, we further investigated the role of ETV5 orchestrating downstream effects to confer the tumor the invasive capabilities needed to disseminate in the early stages of EC dissemination. We demonstrated that ETV5 has a direct role in EMT, and we also identified a number of proteins involved in the acquisition of invasive capabilities by ECs. Furthermore, we postulated lipoma-preferred partner (LPP) as a novel co-regulatory partner of ETV5, in the transcriptional regulation of the EMT process, through a crosstalk with the tumor surrounding microenvironment.

RESULTS

ETV5 promotes EMT in Hec1A cells

The first evidence suggesting that ETV5 transcription factor could be underlying the initial steps of EC invasion came from the endometrial tumor cell line Hec1A resulting in the acquisition of phenotypic characteristics compatible with EMT when the levels of ETV5 expression were increased. Hec1A cells expressed basal levels of nuclear ETV5 while ETV5-overexpressing cells showed in addition the nuclear GFP-fusion protein (see Figure 1 in ref. 22); the former grew in compact colonies with well defined cell–cell contacts, while the later showed a more scattered and individualized fibroblast-like morphology (Figure 1a; see Figure 3 in ref. 21). At the molecular level, massive gene-expression comparison of both cell lines showed that an increase in ETV5 (Figure 1a; Supplementary Table I) was associated with the significant modulation of the expression of 1344 genes ($P<0.001$; $1.3<FC>1.3$). Bioinformatics analysis pointed to cell adhesion, cell–cell contact and cellular junctions, and actin cytoskeleton reorganization as the main cellular functions altered. In addition, cell-to-cell signaling and interaction and cellular movement were the principal biological processes associated with the overexpression of ETV5, reinforcing the linkage of ETV5 with the acquisition of a migratory and invasive phenotype.

Focusing on the expression of well-known markers of EMT, we found elevated levels of N-Cadherin and Fibronectin, while diminished Cyclin D1 expression associated with an increase in ETV5 (Figure 1b; Supplementary Table I). Likewise, and consistent with the observed cell scattered phenotype, genes involved in cellular structures as adherens or tight junctions, desmosomes, hemidesmosomes and focal adhesions such as E-Cadherin, Dysadherin, Catenins, TJPs and Claudins, $\alpha5$ and $\alpha1$ integrins, Plakophilins, Cytokeratins and members of the Immunoglobulin superfamily, appeared altered (Figure 1b; Supplementary Table I). These findings were translated at the protein level, confirming a switch between E-Cadherin and N-Cadherin as the hallmark of EMT associated with increased levels of ETV5, as well as a decrease in β-Catenin, TJP3 or Cytokeratin levels and an increase in Dysadherin and Integrins $\alpha5$ and $\beta1$ (Figures 1c and d). Similar results were obtained in the endometrial tumor cell line Ishikawa, in the presence of increased levels of ETV5 (Supplementary Figure 1A and B). All these data indicated that the increased levels of ETV5 found in ECs associated with myometrial infiltration[17] might be related to EMT and the acquisition of a migratory and invasive phenotype.

To further characterize the role of ETV5 during EMT, we analyzed its capability to regulate genes that have been broadly described as inducers of EMT through the transcriptional regulation of E-Cadherin.[23] We observed an upregulation of Zeb1 and Slug associated with increased levels of ETV5 expression, while weak or no differences were found for other transcriptional regulators as Zeb2 and Snail (Figures1b and 2a; Supplementary Figure 2; Supplementary Table I). Chromatin immunoprecipitation in Hec1A cells demonstrated that ETV5 was able to bind directly to the promoter region of Zeb1, where two ETS-binding sites were identified (Figure 2b). Moreover, ETV5 binding to Zeb1 promoter lead to its transcriptional activation as demonstrated by a marked increase in luciferase activity when the Hec1A cells were transfected with the Zeb1 promoter region containing the ets binding sites-PGL4 reporter vector (Figure 2c). These results demonstrated that ETV5 directly activates Zeb1, a negative regular of E-Cadherin, suggesting a link to the alteration of the cellular architecture associated with EMT.

ETV5 promotes adhesion, migration and invasion in EC cells

We next analyzed whether the molecular and phenotypic features associated with an increased expression of ETV5 were translated into a more aggressive behavior in the EC cells. For this, we assessed changes in cell motility, invasion and adhesion, as those cellular functions are closely related to the initiation of tumor dissemination from a primary carcinoma. Elevated levels of ETV5 expression in the Hec1A cell line implied a high impact on cell invasion as demonstrated in an inverted cell invasion assay mimicking migration through a basement membrane and invasion into an extracellular matrix.[24] Cells expressing increased levels of ETV5 were able to migrate and invade deeply into the matrigel (Figure 3a), with more than 10-fold enhanced invasive competences compared with the parental cell as quantified by RT–qPCR (Figure 3b). Similar results were obtained using the Ishikawa endometrial cell line (Supplementary Figure 1D). Likewise, ETV5 promoted migration of EC cells as measured by transwell-based cell migration assay (Figure 3c), in agreement with previous time-lapse microscopy results.[21] Similar results were obtained when compared with the control GFP-expressing cell line (Supplementary Figure 3).

Hec1A cells expressing increased levels of ETV5 also showed more adhesive capabilities to different ECM substrates, especially to Collagen I (Figure 3d). Related to this, by studying the dynamics of adhesion structures by time-lapse microscopy in cells transfected with Cherry-tagged Paxilin, we found that turnover expressed as time necessary for focal adhesions assembly and disassembly was increased twofold in cells overexpressing ETV5 (Figures 3e and f). The observation that ETV5 both increased the adhesive ability to ECM and the migratory and specially invasive potential of endometrial tumor cells, suggested that a limited gain in cell-matrix adhesive capabilities might be a requisite for enhanced invasive properties, as already described in different model systems.[25,26] These results also confirmed that an increase in ETV5 expression resulted in the acquisition of an aggressive migratory and invasive phenotype in ECs.

LPP cooperates with ETV5 transcription activity

To further characterize the role of ETV5 on EMT and the promotion of migration and invasion, we sought to improve our understanding on how ETV5 was modulated in the context of an invasive EC where transcriptional regulation should respond to the surrounding extracellular signals. For this, we identified proteins associated with endometrial tumor invasion through a two-dimensional differential in gel electrophoresis proteomic approach comparing non-invasive stage IA and highly invasive IB ECs (new FIGO classification; former invasive IC ECs). As mentioned, ETV5 has been described to be specifically upregulated in stage IB ECs.[17] Among those proteins differentially expressed in invasive carcinomas ($P<0.05$; $1.3<FC>1.3$; unpublished results), we identified LPP as one of the most upregulated proteins in invasive carcinomas with a 2,35 fold increase (Figure 4a). LPP is a LIM domain containing protein, which localizes to the cell periphery where it may be involved in cell–cell adhesion and cell motility. LPP has also been described to shuttle through the nucleus where may function as a transcriptional co-activator.[27] Specifically, it has been described as a co-activator of PEA3, a member of the same

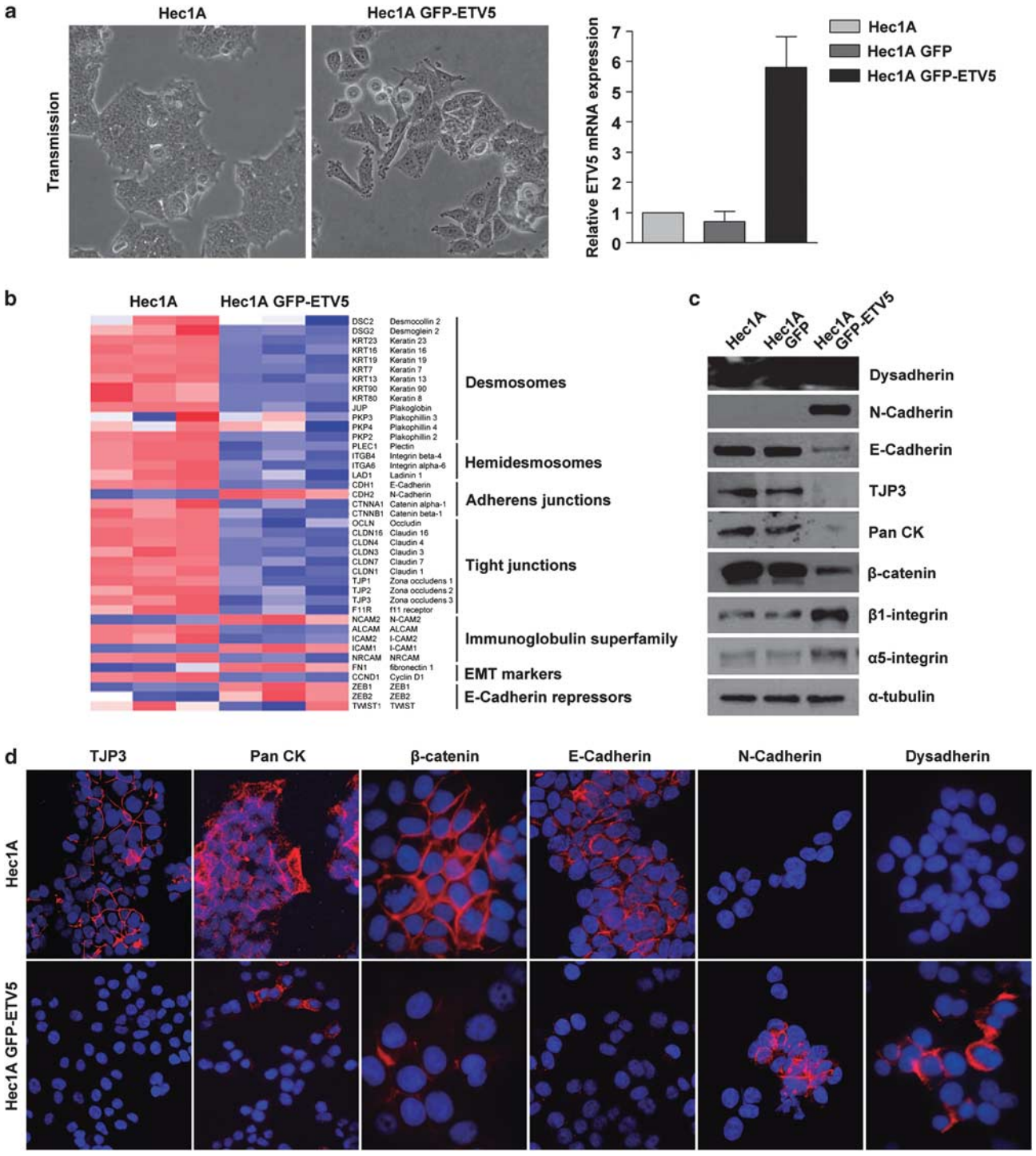

Figure 1. ETV5 induces molecular changes associated with EMT. (**a**) Phase-contrast images showing representative examples of the morphological changes produced by an increase of GFP-ETV5 expression in Hec1A cells. Analysis of mRNA expression by RT-qPCR of ETV5 normalized to 18S as housekeeping gene, in the control parental Hec1A and GFP empty vector-expressing cells, and in the GFP-ETV5-expressing cells (histogram in right panel). (**b**) Heat map of microarray data for three replicates of Hec1A GFP-ETV5 and Hec1A cell lines. Selected genes related with EMT are presented. The key on the top right assigns heat map colors to the absolute gene expression value on a log2 scale. (**c**) Immunoblot analysis with antibodies against proteins related to cell-cell contacts (TJP3 for tight junctions; PanCK for desmosomes; β-Catenin, E- and N-Cadherin and Dysadherin for adherens junctions) and cell-matrix contacts (α5 and β1 integrin for focal adhesions). α-tubulin is used as loading control. Immunoblotting reveals general decrease of cell-cell adhesions components related to EMT transition on ETV5 overexpressing cell line. (**d**) Immunofluorescence staining for TJP3, PanCK, β-Catenin, E- and N-Cadherin and Dysadherin on non-confluent cell cultures. Note epithelial cell-cell adhesion loss concomitant with mesenchymal cell-cell adhesion appearance in cells overexpressing ETV5, whereas opposite effect is observed in Hec1A.

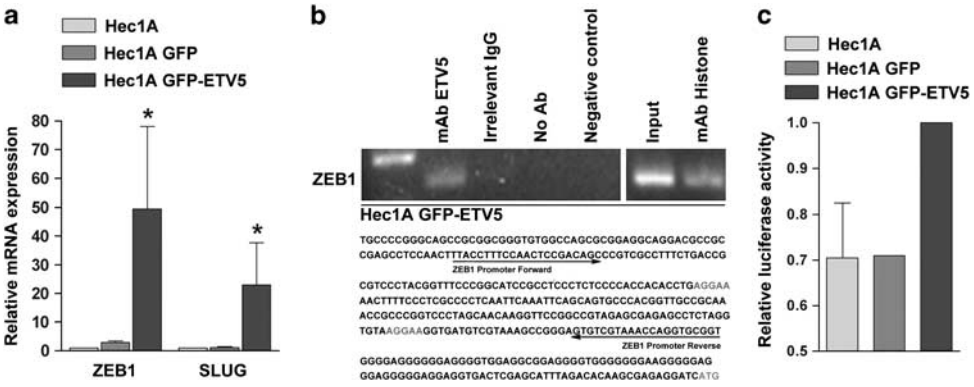

Figure 2. ETV5 induces the expression of E-Cadherin repressors and directly interacts with the promoter region of ZEB1. (**a**) Analysis of mRNA expression by RT–qPCR of known E-Cadherin repressors in Hec1A, Hec1A GFP and Hec1A GFP-ETV5 cells, normalized to GAPDH expression as housekeeping gene. (**b**) Schematic representation of Zeb1 promoter region shows two Ets putative binding sites 5′ to the transcriptional start site (TSS) (in insets). Underlined, forward and reverse primers for the promoter region comprising nucleotides from −343 to −95 to the TSS. PCR analysis of the chromatin immunoprecipitate with antibodies directed against ETV5 shows specific binding to the promoter region of Zeb1. Irrelevant IgGs and negative control, and antibodies directed against the acetylated histone and input are shown as negative and positive controls, respectively. (**c**) ETV5 acts as transcriptional inducer of ZEB1. Hec1A and Hec1A GFP-ETV5 cells were transiently co-transfected with pGL4.15 luciferase reporter vector cloned with the ZEB1 promoter region comprising nucleotides from −495 to −80 to the TSS. Relative luciferase activity is shown. Error bars represent mean ± s.d. of duplicate experiments (*t*-Student's test comparing control cell lines against ETV5 overexpression, $^*P<0.05$).

subfamily of ets transcription factors as ETV5, thus we speculated that LPP could be modulating ETV5 activity in ECs. The upregulation of LPP in invasive endometrial tumors was confirmed by western blotting in an independent series of ECs (Figure 4b). To further evaluate the impact of LPP in the process of EC invasion, we analyzed the ability of the endometrial cell line Hec1A stably expressing increased levels of LPP, to invade the matrigel in the inverted invasion assay. As shown in the sequential images (Figure 4c) and in the RT–qPCR quantification (Figure 4d), LPP promoted cell invasion; thus confirming its active role in EC invasion.

We next performed a detailed analysis of the pattern of expression of ETV5 and LPP in human ECs. For this, we constructed a tissue microarray including normal proliferative and secretory endometrium, atrophic endometrium, simple and complex hyperplasias, and 70 ECs representative of all grades, stages and histological subtypes (see Supplementary Table II). ETV5 showed nuclear localization in the epithelial cells, as expected for a transcription factor, while LPP labeling demonstrated a nuclear and cytoplasmic distribution (Figure 5a). Interestingly, LPP showed a more cytoplasmic than nuclear pattern of staining in normal atrophic endometrium, whereas vice versa in ECs (Figure 5b; histoscore quantification represented in box plots), suggesting a nuclear translocation of LPP associated with endometrial carcinogenesis. Moreover, when we focused on ECs ETV5 and LPP histoscores significantly correlated only at the nuclear staining of the tumor epithelial cells ($P<0.05$, data not shown), indicative of cooperation at the transcriptional level. To further investigate a common role in tumor invasion, we quantified ETV5 and LPP by RT–qPCR at the invasive front of ECs where tumor cells are actively invading the surrounding stroma, compared with their paired superficial zone, where no active invasion is observed. Macroscopically dissected areas of similar percentages of epithelial tumor cells from the superficial zone and from the deep invasive front of 11 primary ECs showed a statistically significant and concomitant increase in ETV5 and LPP expression at the invasive front when normalized against GAPDH as a housekeeping gene ($P<0.05$; Figure 5c). All these evidences suggest that LPP cooperates with ETV5 in the acquisition of an aggressive phenotype at the invasive front of ECs. Interestingly, the expression of the E-Cadherin repressors Zeb1 and Slug was also increased at the invasive front of ECs, translating into the human samples those findings observed in the cell lines (Figure 5c).

The cooperation between ETV5 and LPP at the nuclear level was confirmed by luciferase experiments using a luciferase reporter vector carrying the promoter region of PTGS2, as a known target of ETV5 transcription factor[28] (see Supplementary Figure 4). Hec1A cells overexpressing LPP showed increased ETV5 dependent transcriptional activity compared with cells expressing basal LPP levels (Figure 5d). The translocation of LPP into the nucleus in a context of an active EC invasion might be fostering the transcriptional activity of ETV5 and the promotion of EMT. Interestingly, phenotypic changes promoted by the increased levels of ETV5 in Hec1A cells included the weakening of cell–cell contacts where LPP was located (left panel; Figure 5e), and the re-localization of LPP to focal adhesions (right panel; Figure 5e; see co-localization with the focal adhesion protein Vinculin in Supplementary Figure 5). All these data lead us to hypothesized that, in addition to cooperate in ETV5 transcriptional activity, as a result of the ETV5-dependent transition from an epithelial architecture to a migratory phenotype, the new localization of LPP in focal adhesions might be functioning as an extracellular sensor. This link between cell surface events and ETV5-dependent EMT might exponentially potentiate EC invasion.

LPP acts as a sensor in ETV5-dependent EC invasion

To test this hypothesis we analyzed the behavior of endometrial tumor cells in response to an external invasion promoting signal like EGF, a potent chemoattractive molecule for Hec1A persistent cell invasion (Supplementary Figure 6). We first observed that upon EGF stimulus LPP translocated into the nucleus, immunofluorescence intensity quantification demonstrating a significant shift from cytoplasmic LPP towards nuclear LPP (Figure 6a). Likewise, cytoplasm/nucleus cellular fractionation further confirmed that LPP translocates from the cytoplasmic fraction into the nucleus upon external stimulus with EGF (Figure 6b). We next observed by luciferase experiments using the luciferase reporter vector carrying the promoter region of PTGS2 and in the presence or not of LPP in Hec1A cells with increased levels of ETV5 (Figure 6c), that the silencing of LPP completely eliminated the

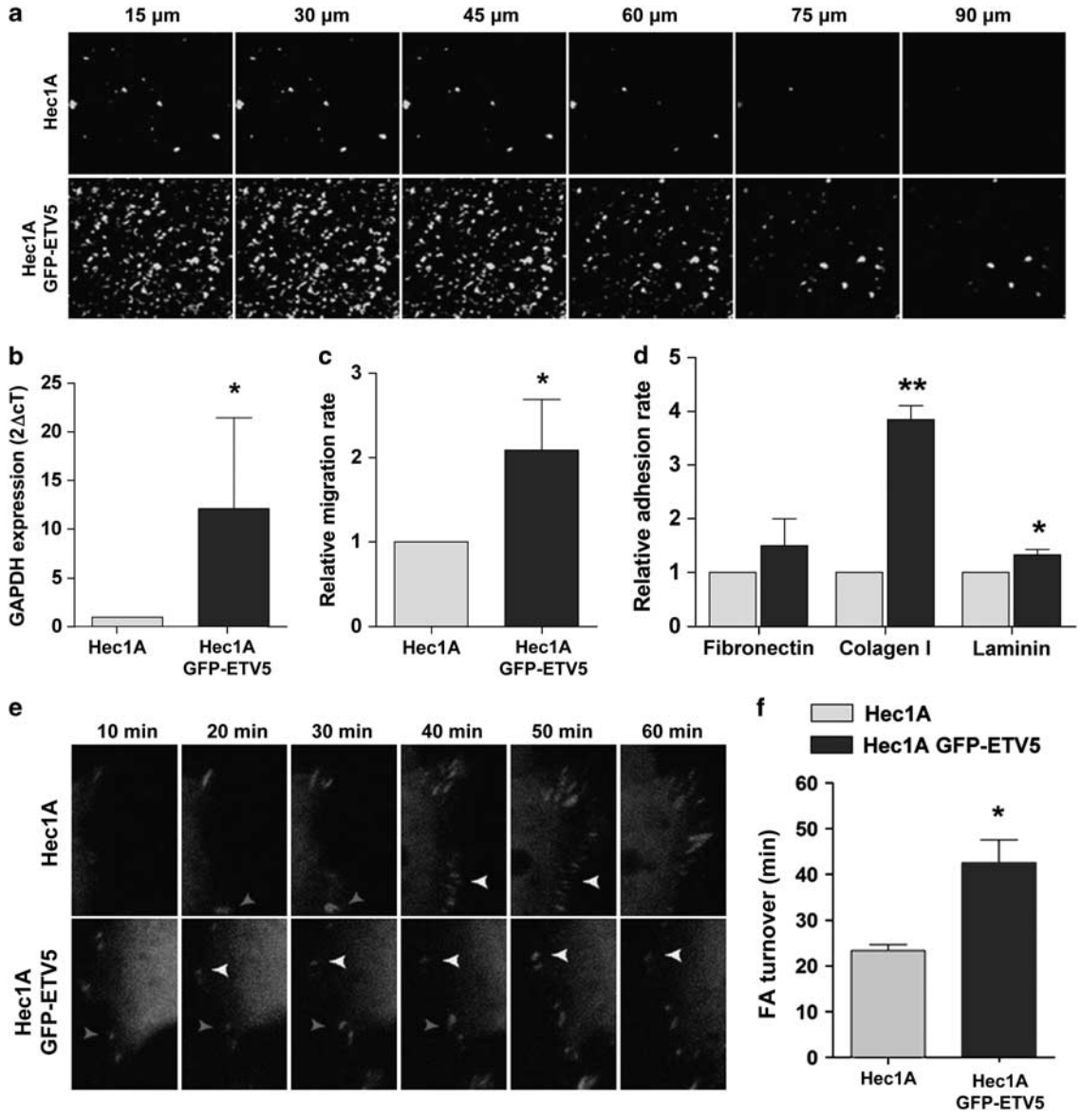

Figure 3. ETV5 influences focal adhesion dynamics and increases adhesion, migration and invasion. (**a**) Image sequence of confocal microscopy sections (15 µm of distance) scanned from the membrane to the top of Matrigel after the inverted invasion assay for both cell types. (**b**) To determine Hec1A invasiveness, GAPDH mRNA levels of cells into Matrigel were employed to quantify the rate of invasion. Data of four independent experiments are represented as fold change (2-ΔCT) in gene expression relative to Hec1A ± s.d. (Mann–Whitney test, $*P<0.05$). (**c**) Cells were seeded at 500 000 cells per well of a 24-well plate and allowed to migrate toward 10% FBS for 48 h. Migratory cells on the bottom of the polycarbonate membrane were quantified in a fluorescence plate reader. Relative migration fluorescence is plot on a bar graph representing mean ± s.d. of three independent experiments (*t*-Student's test, $*P<0.05$). (**d**) Hec1A and Hec1A GFP-ETV5 cells were plated onto coverslips coated with laminin, collagen I and fibronectin. Quantification of ten fields is plot in bar graphs showing media ± s.d. of two independent experiments (*t*-Student's test, $**P<0.001$; $*P<0.05$). (**e**) Focal adhesion dynamics in Hec1A and Hec1A GFP-ETV5 cells are presented with time courses of Cherry–Paxilin. Arrowheads indicate individual focal adhesions that persist for Hec1A GFP-ETV5 cells or that rapidly disappear for Hec1A cells. (**f**) Quantification of focal adhesion turnover rate was carried out from time lapse analysis of images similar to E. Data are summarized in bar graphs showing average time for focal adhesion assembly and disassembly ± s.d. of three independent experiments (*t*-Student's test, $*P<0.05$).

ability of ETV5 expressing cells to response to EGF (Figure 6d). Finally, we evaluated the response to EGF as extracellular signal in the inverted invasion assay by stimulating cells to migrate through the porous membrane and to invade into the matrigel towards the chemoattractive EGF placed on top of the matrigel. Importantly, the almost 30-fold increased invasion observed in Hec1A cells with elevated levels of ETV5 in response to EGF was completely abrogated when LPP was silenced by short hairpin RNA (Figure 6e). Interestingly, Hec1A cells presenting basal ETV5 but increased LPP expression did not augmented significantly their response to EGF (data not shown). This is consistent with the augmented expression of both proteins found at the invasive front of ECs being necessary for an exponentially increased carcinoma invasion. These results reinforced the conclusion that both proteins cooperatively act in the promotion of EC invasion in response to external stimuli.

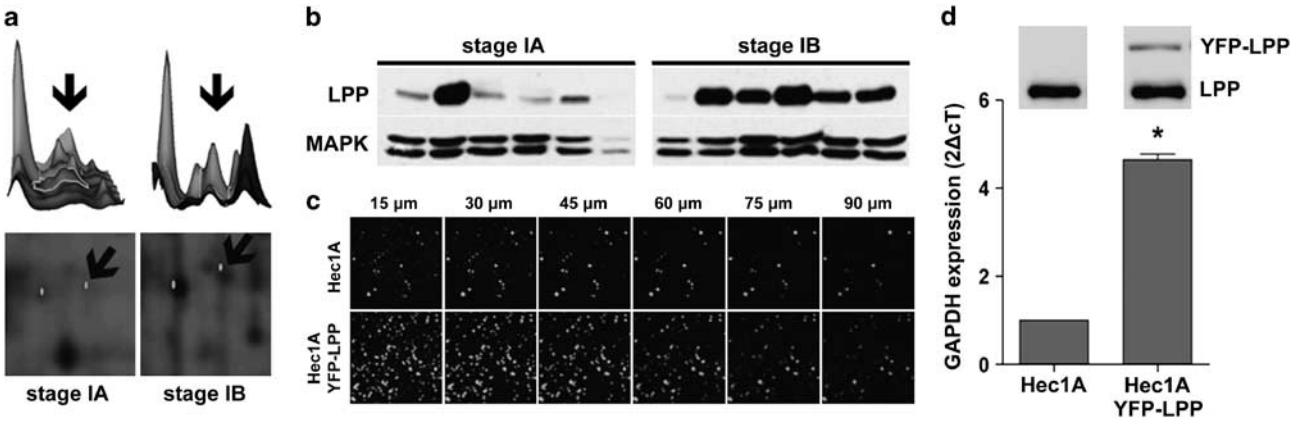

Figure 4. LPP is upregulated in invasive EC and promotes invasion. (**a**) LPP detection by two-dimensional differential in gel electrophoresis (2D-DIGE) analysis comparing protein extracts from non-invasive ($n=4$) and invasive ($n=5$) ECs tissues. (**b**) Immunoblot detection of human LPP protein in stage IA ($n=6$) and IB ($n=6$) human EC tissue samples validates DIGE analysis. MAPK was blotted as loading control. (**c**) Hec1A cells overexpressing YFP-LPP and Hec1A cell line were seeded into an inverted invasion assay and allowed to migrate towards 10% FBS for 2 weeks. Confocal microscopy images were scanned every 15 µm from the membrane to the top of Matrigel. (**d**) To determine cell invasiveness, GAPDH mRNA levels corresponding to cells into Matrigel were determined to quantify the rate of invasion. Data of three independent experiments are represented as fold change (2-ΔCT) in gene expression relative to Hec1A ± s.d. (Mann–Whitney test, $*P<0.05$). On top, immunoblot against LPP demonstrates LPP overexpression.

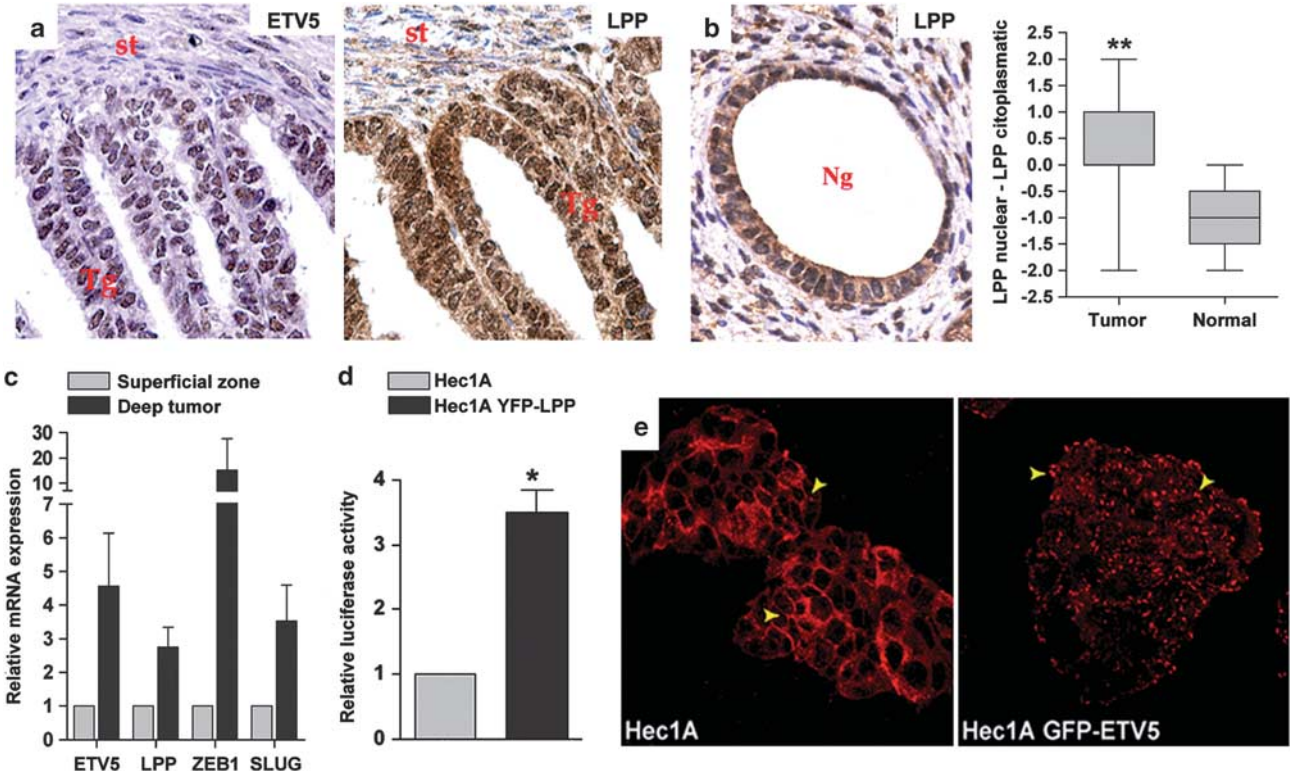

Figure 5. LPP localizes to the nucleus and cooperates with ETV5 in invasion in a transcriptional level and is relocalized to focal adhesions. (**a**) Tissue-array images representative of endometrial tissue microarray (TMA) analysis of ETV5 and LPP protein expression by immunohistochemistry. Note the nuclear staining concomitant for both proteins in tumoral epithelial cells (st, stroma; Tg, tumoral gland). (**b**) Immunohistochemistry showing intense LPP cytoplasmic, whereas weak LPP nuclear staining in normal epithelial glands (Ng, normal gland). Histogram representing the shift in cytoplasmic versus nuclear LPP staining from normal to tumor epithelial glands included on the TMA (*t*-Student's test; $**P<0.001$). (**c**) Histogram representing the relative expression of ETV5, LPP, ZEB1 and SLUG in endometrial tumors comparing superficial zone ($n=11$) against deep invasive front ($n=11$) determined by RT-qPCR. Results are plot as the average fold change (2-ΔCT) ± s.d. relative to the superficial tumor zone (Wilcoxon test; $*P<0.05$). (**d**) Hec1A and Hec1A YFP-LPP cells were transiently co-transfected with PGL3 luciferase reporter vector containing PTGS2 promoter region. Relative luciferase activity to Hec1A data are shown. Error bars represent mean ± s.d. of duplicate experiments (*t*-Student's test; $*P<0.05$). (**e**) Immunofluorescence staining for LPP on non-confluent cell cultures. Note arrow heads indicating LPP localization in cell–cell contacts in Hec1A cells (left panel) and relocalization to focal adhesions in Hec1A GFP–ETV5 (right panel).

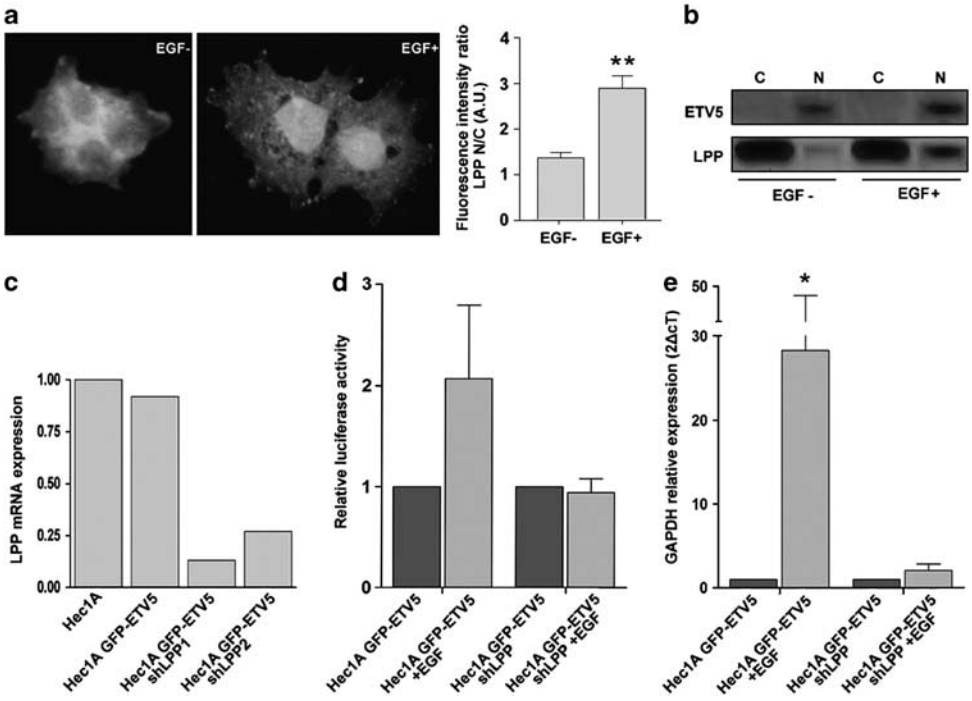

Figure 6. LPP amplifies external EGF stimuli to promote ETV5 downstream effects. (**a**) Confocal immunofluorescence showing LPP staining in the absence (left panel) or presence (right panel) of EGF as external stimulus for migration/invasion. Histogram of fluorescence intensity ratios between nuclear and cytoplasmic LPP in the absence or presence of EGF (**$P<0.001$). (**b**) Western-blot analysis of nuclear and cytoplasmic LPP in the absence or presence of EGF processed for cellular fractionation. ETV5 transcrition factor was used as marker of nuclear fraction. (**c**) Analysis of mRNA expression by RT–qPCR of LPP demonstrates its inhibition in two different LPP inhibition stable clones of Hec1A cells overexpressing ETV5 (shLPP1 and shLPP2). 18S expression is analyzed as loading control. (**d**) Hec1A GFP–ETV5 (HGE) cells and shLPP1 and 2 were transiently co-transfected with PGL3 luciferase reporter vector cloned with PTGS2 promoter region. Cells were untreated or treated with EGF (60 ng/ml) for 16 h before measuring luciferase. Relative luciferase activity to non-treated cells data are shown. Error bars represent mean ± s.d. of two independent experiments. (**e**) HGE cells and shLPP1 and 2 were seeded into an inverted invasion assay and allowed to migrate towards 10% FBS for 2 weeks. Cells were untreated or treated with EGF (60 ng/ml) for the whole experiment period. GAPDH mRNA level of cells into Matrigel was determined to quantify the rate of invasion. Data from four independent experiments are represented as fold change (2-ΔCT) in gene expression relative to non-treated cells ± s.d. (Mann–Whitney test, *$P<0.05$).

DISCUSSION

Myometrial infiltration remains one of the most important prognostic factors associated with 5-year survival in endometrial cancer.[29] In this work we depicted the role of the Ets transcription factor ETV5 in EC invasion by its direct transcriptional induction of the EMT process and its ability to cross-talk with the environment through its cooperation with LPP. ETV5 has been identified in a gene expression profiling analysis as specifically upregulated in invasive ECs,[17] associated with its capability to regulate mediators of the myometrial infiltrative process.[21,22] The findings presented here emphasize its critical role in the early stages of invasion of EC, as we now describe a principal function for ETV5 transcription factor in the promotion of EMT. We first characterized at the molecular level the alterations associated with the acquisition of a mesenchymal phenotype, and depicted a main regulatory effect of ETV5 by modulating E-Cadherin repression. Loss of E-Cadherin has been broadly studied and is considered the hallmark of EMT.[30] We further demonstrated that ETV5 transcriptionally activates the zinc finger E-box-binding transcription factor Zeb1, an important E-Cadherin repressor.[10] High levels of Zeb1 have been described to encourage gynecologic carcinoma progression,[31] and an interplay between transcriptional repressors of E-Cadherin and miRNAs has been linked to EMT-activation in human ECs.[32]

EMT endows cells not only with migratory and invasive properties, but induces stem cell properties, prevents apoptosis and senescence, and contributes to immunosuppression. The mesenchymal state is associated with the capacity of cells to migrate to distant organs and maintain stemness, allowing their subsequent differentiation into multiple cell types during development and the initiation of metastasis.[33] Functionally, the transition to a mesenchymal phenotype upon an increase in ETV5 expression resulted in the acquisition of migratory capabilities, in accordance to previous results.[21] Importantly, the invasive properties of cells presenting increased levels of ETV5 were significantly potentiated resulting in an effective and collective directional invasion in a three-dimensional *in vitro* assay that mimics human carcinoma invasion. In addition, ETV5 overexpressing cells became more adhesive, compatible with the premise that cells need to adhere previous to further invade in order to improve the efficacy of this initial step in the process of metastasis.[25,26]

However, it is not only the increased adhesion and invasive capabilities of transformed cells what is needed for a successful progression of the tumor, but also, the capability of those cells to communicate and understand the signals of the surrounding microenvironment.[34] Interestingly, our studies in ovarian cancer demonstrated that ETV5 upregulation induced rather than repressed the expression of cell adhesion molecules to enhance cell survival in a spheroid model.[35] The ETV5-dependent upregulation of E-Cadherin may facilitate transcoelomic ovarian cancer dissemination, highlighting the plasticity of tumor cells and their capacity to modulate the regulatory pathways of EMT in response to particular requirements imposed by specific tumor environments. The adaptive transcriptional program of ETV5

during the initial steps of dissemination at least in gynecological carcinomas, suggests the active participation of co-regulatory proteins that are capable to correctly interpret the tumor environment. Through a proteomic approach performed in invasive and non-invasive ECs, we found LPP significantly associated with myometrial infiltration. LPP is a LIM domain containing preferred translocation partner in lipoma (LPP) that has been proposed previously to ensure a dual function at the cell periphery and in the nucleus.[36] LPP binds actin-interacting proteins, localizes to the cell periphery in focal adhesions and may be involved in cell–cell adhesion and cell motility.[37] Our data in the 3-D *in vitro* invasion assay confirmed a role for LPP in EC invasion. LPP has also been described to shuttle through the nucleus and may function as a transcriptional co-activator.[27,36] In particular, it has been described as a co-activator of PEA3, a member of the same subfamily of ets transcription factors as ETV5. Our analysis pointed to a cooperation of both proteins in the invasive capabilities of ECs.

Interestingly, the EMT promoted by ETV5 resulted in the localization of LPP from cell–cell contacts to focal adhesions, and this was translated into an increase in ETV5 transcription activity that finally resulted in a feedback loop mechanisms, where ETV5 promoted further invasion. Compatible with these data, we demonstrated a link between ETV5 and LPP in response to extracellular signals in the promotion of carcinoma invasion. Orchestrated modulation of cell adhesion is essential for appropriate cell responses and intercellular communication. In tumor cell biology, dynamic control of adhesion molecules is important to proceed through the metastatic cascade and to allow cell release from the primary tumor, invasion of the surrounding matrix, intravasation and adhesion to vascular endothelial cells to facilitate extravasation. In addition, focal adhesion proteins may function as a cell surface sensor to regulate cellular signaling and dynamic responses.[38] Likewise, deletion of focal adhesion kinase impairs directed migration in endothelial cells,[39] and its activation is required by both attractive and repulsive cues to control, respectively, axon outgrowth and disassembly of adhesive structures together with cytoskeletal dynamics.[40] Our model of EC invasion postulates that increased levels of ETV5 are translated into a transcriptional promotion of EMT (Figure 7a). In a second step, EMT results in the localization of LPP at focal adhesions, where extracellular signals are amplified by its translocation to the nucleus and a further activation of ETV5 transcription activity. This amplification loop resulted in a deep persistent EC invasion (Figure 7b).

From a clinical point of view, tumor invasion defines the frontier between tissue-restricted carcinoma and disseminated tumor cells. The former represents good outcome as optimal surgery, the best therapeutic alternative now-a-days, becomes possible. The latter is associated with poor prognosis and a dramatic decreased in survival, with therapeutic options based on radiotherapy and chemotherapy showing limited efficacy and being still a promise when dissemination and metastasis are present. Therefore, understanding the molecular events related to myometrial infiltration and distant metastasis represents a decisive requirement for the design of new therapeutic approaches against the most devastating points in endometrial cancer.

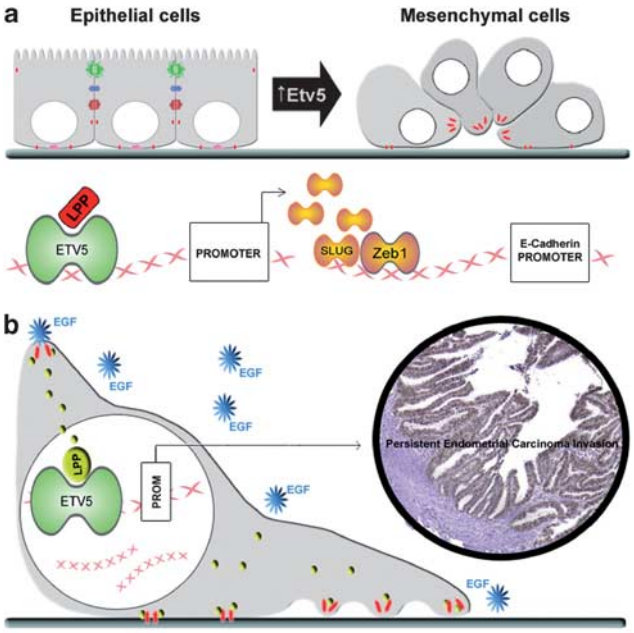

Figure 7. Schematic representation of a novel model for ETV5 transcription factor in EC invasion. (**a**) Upper part illustrates EMT. Starting from the left, we observe epithelial cells maintaining polarity and cell–cell contacts upon ETV5 upregulation. ETV5 leads to a functional switch towards the mesenchymal phenotype and behavior, represented on the right, by more aggressive cells that have dissolved cell–cell contacts and have increased invasive and migratory capabilities. Lower part focuses on ETV5 transcriptional regulation to induce E-Cadherin repression, as hallmark of the EMT process. In our model, ETV5 binds to Zeb1 promoter region and induces its expression. As Zeb1 is a known repressor of E-Cadherin, its increased expression would decrease E-Cadherin transcription and so, the switch between E- and N-Cadherin may occur and EMT triggered. (**b**) Invasion into surrounding tissues is further studied by understanding the relation between mesenchymal cells and stimuli received by the environment. Our working model of the molecular mechanisms underlying the change in LPP subcellular localization and its interacting partner ETV5 during EMT is depicted. In mesenchymal cells, LPP is relocalized to focal adhesions to function as an extracellular sensor. In front of extracellular stimuli, LPP is needed to activate a response through its own translocation to the nucleus and cooperation with ETV5 on controlling transcription, which leads to persistent invasion on EC.

MATERIALS AND METHODS

Cell lines, constructs and stable cell lines generation

The human EC cell lines, Hec1A and Ishikawa, were cultured in McCoys 5A medium with GlutaMAX (Life Technologies, Grand Island, NY, USA) and DMEM:F12 (GIBCO, Invitrogen, Carlsbad, CA, USA), respectively. Both supplemented with 10% fetal bovine serum. Cell lines either transfected with the pEGFP-C2 vector alone (Hec1A GFP) or the hERM/ETV5 (Hec1A GFP-ETV5 and Ishikawa GFP-ETV5) were constructed and selected with G-418 as described.[21] Stable short hairpin RNA (5′-TCCACCTGCTGACGAATAC-3′ sequence) and YFP–LPP constructs were stably transfected in order to knock-down and upregulate LPP expression, respectively. Transfection was carried out using Lipofectamine 2000 (Invitrogen, Carlsbad, CA, USA) according to manufacturer conditions and cells were selected with Puromycin B (InvivoGen, San Diego, CA, USA) at a concentration of 1 μg/ml and G-418 as described in ref. 21. Two different clones were obtained for LPP knockdown expression in the Hec1A GFP–ETV5 cell line (shLPP1 and shLPP2) and the results of both are plotted together as shLPP.

Western-blot and cellular fractionation

Protein lysates from tissues of six independent stage IA and stage IB (former IC stage) ECs were obtained as described.[41] Cell lysates were obtained by scratching with RIPA buffer (Tris 20 mM pH8.8, NaCl 150 mM, EDTA 5 mM, Triton X-100 1%, protease inhibitors) and supernatant boiled with Laemmli buffer. Samples were separated on SDS–PAGE gels, transferred onto a nitrocellulose membrane (BioRad, Hercules, CA, USA) and incubated with primary antibodies at 4 °C overnight (1:1000 mAb α-N-Cadherin, BD Transduction Laboratories, Palo Alto, CA, USA; 1:2000 mAb α-

E-Cadherin, BD Transduction Laboratories; 1:1000 mAb α-TJP3, Abnova; 1:500 mAb α-β-catenin, BD Biosciences; 1:500 α-Dysadherin from NCC-M53 (Shimamura *et al*., 2003); 1:200 mAb α-PanCK AE1/AE3, Novocastra, Leica Microsystems, Wetzlar, Germany; 1:2500 rAb α-Integrin α1, BD Transduction Laboratories; 1:500 rAb α-Integrin α5, Millipore, Billerica, MA, USA; 1:200 rAb α-PARP, Cell Signalling, Beverly, MA, USA; 1:100 rAb α-LPP, ImmunoGlobe, Himmelstadt, Germany; 1:100 rAb α-ERM/ETV5, Santa Cruz Biotechnology, Santa Cruz, CA, USA; 1:2000 rAb α-Tubulinα, Cell Signalling; 1:2000 rAb α-Mapk, Signalling). Proteins were revealed with HRP-conjugated rabbit anti-mouse and goat anti-rabbit immunoglobulins (DAKO, Glostrup, Denmark) and the Millipore Immobilon Western Chemiluminescent HRP Substrate (Millipore).

Alternatively, Hec1A GFP-ETV5 cells were treated with EGF (60 ng/ml) for 6 h, washed in PBS and incubated in hypotonic buffer (10 mM HEPES, 1 mM EDTA, 1 mM EGTA, 1 mM DTT, 10 mM KCl, 0,5% NP-40 and protease inhibitors, pH 7.9) for 10 min. Cytoplasmic fractions were obtained by centrifugation at 1500 *g* for 15 min. Pellets were washed twice and homogenized in a buffer composed of 10 mM HEPES, 1 mM EDTA, 1 mM EGTA, 1 mM DTT, 0,4 M KCl, 20% glycerol and protease inhibitors for 30 min. Supernatants containing nuclear proteins were obtained by centrifugation at 25000 *g* for 15 min.

Immunofluorescence and imaging

For detection of LPP, Dysadherin, Vinculin, β-catenin, TJP3, PanCK, E- and N-Cadherin, cells were seeded onto glass coverslips, fixed with 4% paraformaldehyde for 10 min and permeabilized with PBS Triton X-100 4% for 10 min. Cells were sequentially incubated with primary and secondary antibodies conjugated with 568-alexa fluor (Molecular Probes, Invitrogen, Carlsbad, CA, USA) for 1 h at RT in dark. Coverslips were mounted using the Aqua/Poly Mount medium (Polysciences Europe GmbH, Eppelheim, Germany). Transmission images were captured using FSX100 microscope (Olympus, Hamburg, Germany) and fluorescence images were captured with DM-IRBE inverted fluorescence microscope (Leica, Wetzlar, Germany) coupled to a TCS-NT argon/krypton confocal laser (Leica). Z-stacks collected for LPP imaging upon stimulus with EGF were averaged projected and the fluorescence intensity was quantified with the Leica Confocal Software.

Semiquantitative RT-PCR and Quantitative RT-PCR

Total RNA from cell cultures and tissues was obtained using the RNeasy Mini kit (Qiagen, Valencia, CA, USA). cDNA synthesis was performed using SuperScript III reverse transcription enzyme (Invitrogen). Quantitative real-time PCR (RT-qPCR) was done as described previously[17] with TaqMan probes against ETV5 (Hs00231790_m1), LPP (Hs00194400_m1), SLUG (Hs00950344_m1), ZEB1 (Hs00232783_m1), 18S ribosomal RNA (4319413E-0406012) and GAPDH (Hs99999905_m1) (Applied Biosystems, Foster City, CA, USA). GAPDH and 18S were used to normalize.

cDNA microarrays

Microarrays were carried out using the Affymetrix microarray platform and the Genechip Human Gene 1.0 ST Array (Affymetrix, Santa Clara, CA, USA). This array analyzes gene expression patterns on a whole-genome scale on a single array with probes covering many exons on the target genomes, and thus permitting expression summarization at the exon level. Triplicates of Hec1A and Hec1A GFP ETV5 were used to perform this study. Starting material was 100 ng of total RNA of each sample. Quality of isolated RNA was first measured by Bioanalyzer Assay (Agilent, Santa Clara, CA, USA). Briefly, sense ssDNA suitable for labeling was generated from total RNA with the Ambion WT Expression Kit from Ambion (Austin, TX, USA) according to the manufacturer's instructions. Sense ssDNA was fragmented, labeled and hybridized to the arrays with the GeneChip WT Terminal Labeling and Hybridization Kit from Affymetrix (Affymetrix). Chips were processed on an Affymetrix GeneChip Fluidics Station 450 and Scanner 3000. Images were processed with Microarray Analysis Suite 5.0 (Affymetrix). All samples demonstrated characteristics of high-quality cRNA and were subjected to subsequent analysis. Raw expression values were preprocessed using the RMA method.[42] Data were submitted to non-specific filtering to remove low signal genes and low variability genes. The selection of differentially expressed genes between conditions was based on a linear model analysis with empirical Bayes moderation of the variance estimates following Smyth methodology.[43] The analysis yields standard tests statistics such as fold changes or *P*-values, which are used to determine differentially expressed genes. All the statistical analysis was done using the free statistical language R and the libraries developed for microarray data analysis by the Bioconductor Project. Differentially expressed genes related to structures and mechanisms involved in the EMT are ploted on a heatmap and its data are shown in clusters.

Chromatin immunoprecipitation assay

Chromatin immunoprecipitation on Hec1A GFP-ETV5 cells against ETV5 antibody (Santa Cruz Biotechnology) was done as per manufacturer's recommendations using Magna chromatin immunoprecipitation A (Millipore). Total input and DNA immunoprecipitated with rAb α-acetyl-histone H3 were used as positive controls and DNA immunoprecipitated with α-normal rabbit IgGs and non-antibody were used as negative controls. For PCR analysis, 1 μl of input DNA extraction and 5 μl of immunoprecipitated DNA were used for 35 cycles of amplification at 60 °C of annealing temperature. The primers for Zeb1 promoter region covered the sequence between −343 and −95 from the transcriptional start site, and were designed as follows: forward, 5′-TTACCTTTCCAACTCCGACAG-3′ and reverse, 5′-CCGCACCTGGTTTACGACAC-3′.

Adhesion assay

5×10^4 cells were seeded into fibronectin-, laminin- and colagen I-coated coverslips and allowed to adhere between 20 and 40 min depending on the matrix. Adherent cells were fixed and stained with 1:1000 dapi and 1:200 phalloidin. At least five random fields per coverslips were manually quantified using the FSX100 microscope (Olympus). All experiments were done in triplicate. Measurements were made in at least two independent experiments. *T*-test statistical analysis was performed with SPSS 16.0 software (SPSS, IBM, Armonk, NY, USA). Differences between the groups were considered significant if the *P*-value was <0.05.

Transwell migration assay

5×10^5 cells were seeded on 8 μm pore size transwell filters of the CytoSelect 24-well cell migration assay kit (Cell Biolabs, San Diego, CA, USA), and allowed to migrate for 48 h. Cells were quantified according to the manufacturer's protocol. Measurements were made in three independent experiments. *T*-test statistical analysis was performed with SPSS 16.0 software (SPSS). Differences between the groups were considered significant if the *P*-value was <0.05.

Focal adhesion turnover analysis

Cells were transiently transfected with Cherry-Paxilin, a construct kindly donated by Dr Vignjevic. After 24 h of transfection, cells were plated onto 18 mm fibronectin-coated coverslips and allowed to adhere for 48 h. The coverslips were then mounted in a Ludin Chamber (Life Imaging Services, Basel, Switzerland) with L15 medium without phenol red (Invitrogen) supplemented with 10% FBS and placed in a 37 °C heated chamber. Images were collected with the ×40 objective of an inverted microscope (TE2000-U; Nikon, Tokyo, Japan) equipped with a spinning disk head (CSU; Yokogawa, Tokyo, Japan) and a charge-coupled device camera (CoolSNAP HQ2; Photometrics, Tucson, AZ, USA) and operated with MetaMorph 7.1.4 (MDS Analytical Technologies, Berkshire, UK). Fluorescence images were taken every 2-5 min for Cherry-Paxilin. Focal adhesion turnovers were analyzed by counting the time lapsed between the first and last frames in which a focal adhesion was observed. Measurements were made in three independent experiments. *T*-test statistical analysis was performed with SPSS 16.0 software (SPSS). Differences between the groups were considered significant if the *P*-value was <0.001.

Cell inverted invasion assay

Invasion assay was performed as previously described by Muinelo Romay.[24] Briefly, cells were seeded at 5×10^5 cells/ml directly onto the opposite face of the 8 μm size pore membrane transwell (Corning, Lowell, MA, USA) and incubated for 5 h before turning right-side-up. Diluted matrigel growth factor-reduced (BD Bioscience, Franklin Lakes, NJ, USA) was placed over the upper well. Inserts were placed in serum-free medium while 10% FBS complemented medium was applied on top of the Matrigel. hEGF (60 ng/ml) (Sigma, St Louis, MO, USA) was used as chemoattractant on the upper face of the insert. Living cells were stained with 4 μM of calcein-acetoxymethyl ester (Invitrogen) and visualized by confocal microscopy after 15 days. Images were scanned every 5 μm intervals using a $\times 10$ objective. mRNA extraction from cells invading into the matrigel were extracted and quantified by RT–qPCR using the protocol previously described.[24]

Luciferase assay

The human Zeb1 promoter cloned in PGL4.15 and the mouse PTGS2 promoter cloned in PGL3 luciferase vectors were generous gifts from Dr Min Yu and Dr D DeWitt, respectively. Cells were split into 24-well plates before transfection and were transfected with a mixture of 370 ng reporter luciferase vector, 30 ng renilla luciferase vector and Lipofectamine 2000 (Invitrogen) for 5 h with serum-free media. The transfection mixture was replaced with complete media with or without growth factor stimuli: 60 ng/ml hEGF (Sigma), 100 pM TGFβ (R&D Systems, Minneapolis, MN, USA), 100 ng/ml IGFII (Sigma) and 100 ng/ml bFGF (Roche, Basel, Switzerland) were used according to manufacturer's instructions. After 36 h, cells were lysed and luciferase activity determined using Dual Luciferase Assay Kit (Promega, Madison, WI, USA). Data are presented as relative fold activation from at least two independent transfection experiments. *T*-test statistical analysis was performed with SPSS 16.0 software (SPSS). Differences between the groups were considered significant if the *P*-value was <0.05.

Two-dimensional differential in gel electrophoresis

Sample preparation, two-dimensional differential in gel electrophoresis and protein identification by mass spectrometry were done as described previously.[22] Image analysis and statistical quantification of relative protein abundances were performed using DeCyder V. 6.0 software (GE Healthcare, Waukesha, WI, USA). Protein features were selected by presenting *t*-test values $\leqslant 0.05$, when comparing five invasive stage IB EC tissues (former IC stage) with four stage IA EC tissues, together with a fold-change $> \pm 1.3$.

Tissue Microarray

Two tissue microarrays were constructed at the Pathology Department of the Vall d'Hebron University Hospital. Representative areas from 69 paraffin-embedded tissues from different types and grades of carcinomas and controls (Supplementary Table II) were carefully selected and marked on individual paraffin blocks. Two tissue cores of 1 mm in diameter were obtained from each paraffin block and were precisely arrayed in a new paraffin block. Sections of 5 μm were obtained from all tissue microarray paraffin blocks. LPP and ETV5 were detected by the indirect immunoperoxidase assay with citrate buffer pH 7.3 and 9, respectively, for antigen retrieval. Sections were incubated with primary antibodies from 1 to 2 h at room temperature using a dilution 1:100. Thereafter sections were incubated with peroxidase conjugated goat anti-rabbit immunoglobulin (EnVision Dual System, DAKO). Endogenous peroxidase activity was quenched with 3% H_2O_2. Sections were washed, and reactions were developed with diaminobenzidine, followed by counterstaining with hematoxylin. Semiquantitative evaluations of both proteins were performed by an experienced pathologist, scoring the intensity of the staining and its localization. The quantity of positive immunostaining was evaluated as follows: 1-low, 2-medium, and 3-high.

CONFLICT OF INTEREST

The authors declare no conflict of interest.

ACKNOWLEDGEMENTS

This work was supported by the Spanish Ministry of Science and Innovation (SAF 2005-06771; SAF 2008-03996), Spanish Ministry of Health (RTICC RD06/0020/0058; CP08/00142, PI08/0797), European Commission Program Fondo Europeo de Desarrollo Regional (FEDER), Catalan Institute of Health (DURSI 2005SGR00553), Fundacio La Marato de TV3 (grant 050431), ACCIO (RDITSCON07-1-0001), AECC (Grupos Estables de Investigacion 2011) and National Programme of Biotecnology (FIT-010000-2007-26). LAA and JB are recipients of fellowships from the Basque Government (Spain) and the Spanish Ministry of Education and Science, respectively.

REFERENCES

1 Jemal A, Siegel R, Xu J, Ward E. Cancer statistics, 2010. *CA A Cancer J Clinicians* 2010; **60**: 277–300.
2 Abal M, Llaurado M, Doll A, Monge M, Colas E, Gonzalez M *et al.* Molecular determinants of invasion in endometrial cancer. *Clin Transl Oncol* 2007; **9**: 272–277.
3 Radisky DC, Kenny PA, Bissell MJ. Fibrosis and cancer: do myofibroblasts come also from epithelial cells via EMT? *J Cell Biochem* 2007; **101**: 830–839.
4 Thiery JP, Sleeman JP. Complex networks orchestrate epithelial-mesenchymal transitions. *Nat Rev Mol Cell Biol* 2006; **7**: 131–142.
5 Kalluri R, Zeisberg M. Fibroblasts in cancer. *Nat Rev Cancer* 2006; **6**: 392–401.
6 Thiery JP, Morgan M. Breast cancer progression with a Twist. *Nat Med* 2004; **10**: 777–778.
7 Kang Y, Massague J. Epithelial-mesenchymal transitions: twist in development and metastasis. *Cell* 2004; **118**: 277–279.
8 Mueller MM, Fusenig NE. Friends or foes - bipolar effects of the tumour stroma in cancer. *Nat Rev Cancer* 2004; **4**: 839–849.
9 Bhowmick NA, Neilson EG, Moses HL. Stromal fibroblasts in cancer initiation and progression. *Nature* 2004; **432**: 332–337.
10 Peinado H, Olmeda D, Cano A. Snail, Zeb and bHLH factors in tumour progression: an alliance against the epithelial phenotype? *Nat Rev Cancer* 2007; **7**: 415–428.
11 Nieto MA. The snail superfamily of zinc-finger transcription factors. *Nat Rev Mol Biol* 2002; **3**: 155–166.
12 Peinado H, Portillo F, Cano A. Transcriptional regulation of cadherins during development and carcinogenesis. *Int J Dev Biol* 2004; **48**: 365–375.
13 Yang J, Mani SA, Donaher JL, Ramaswamy S, Itzykson RA, Come C *et al.* Twist, a master regulator of morphogenesis, plays an essential role in tumor metastasis. *Cell* 2004; **117**: 927–939.
14 Yang J, Weinberg RA. Epithelial-mesenchymal transition: at the crossroads of development and tumor metastasis. *Dev Cell* 2008; **14**: 818–829.
15 Sivridis E. Angiogenesis and endometrial cancer. *Anticancer Res* 2001; **21**: 4383–4388.
16 Tsukamoto H, Shibata K, Kajiyama H, Terauchi M, Nawa A, Kikkawa F. Uterine smooth muscle cells increase invasive ability of endometrial carcinoma cells through tumor-stromal interaction. *Clin Exp Metastasis* 2007; **24**: 423–429.
17 Planaguma J, Abal M, Gil-Moreno A, Diaz-Fuertes M, Monge M, Garcia A *et al.* Up-regulation of ERM/ETV5 correlates with the degree of myometrial infiltration in endometrioid endometrial carcinoma. *J Pathol* 2005; **207**: 422–429.
18 Planaguma J, Diaz-Fuertes M, Gil-Moreno A, Abal M, Monge M, Garcia A *et al.* A differential gene expression profile reveals overexpression of RUNX1/AML1 in invasive endometrioid carcinoma. *Cancer Res* 2004; **64**: 8846–8853.
19 de Launoit Y, Baert JL, Chotteau-Lelievre A, Monte D, Coutte L, Mauen S *et al.* The Ets transcription factors of the PEA3 group: transcriptional regulators in metastasis. *Biochim Biophys Acta* 2006; **1766**: 79–87.
20 Graves BJ, Petersen JM. Specificity within the ets family of transcription factors. *Adv Cancer Res* 1998; **75**: 1–55.
21 Monge M, Colas E, Doll A, Gonzalez M, Gil-Moreno A, Planaguma J *et al.* ERM/ETV5 up-regulation plays a role during myometrial infiltration through matrix metalloproteinase-2 activation in endometrial cancer. *Cancer Res* 2007; **67**: 6753–6759.
22 Monge M, Colas E, Doll A, Gil-Moreno A, Castellvi J, Diaz B *et al.* Proteomic approach to ETV5 during endometrial carcinoma invasion reveals a link to oxidative stress. *Carcinogenesis* 2009; **30**: 1288–1297.
23 Thuault S, Valcourt U, Petersen M, Manfioletti G, Heldin CH, Moustakas A. Transforming growth factor-beta employs HMGA2 to elicit epithelial-mesenchymal transition. *J cell Biol* 2006; **174**: 175–183.
24 Muinelo-Romay L, Colas E, Barbazan J, Alonso-Alconada L, Alonso-Nocelo M, Bouso M *et al.* High risk endometrial carcinoma profiling identifies TGF-{beta}1 as a key factor in the initiation of tumor invasion. *Mol Cancer Ther* 2011; **10**: 1357–1366.
25 Sawada K, Mitra AK, Radjabi AR, Bhaskar V, Kistner EO, Tretiakova M *et al.* Loss of E-cadherin promotes ovarian cancer metastasis via alpha 5-integrin, which is a therapeutic target. *Cancer Res* 2008; **68**: 2329–2339.

26 Stoletov K, Kato H, Zardouzian E, Kelber J, Yang J, Shattil S *et al.* Visualizing extravasation dynamics of metastatic tumor cells. *J Cell Sci* 2010; **123**: 2332 - 2341.
27 Guo B, Sallis RE, Greenall A, Petit MM, Jansen E, Young L *et al.* The LIM domain protein LPP is a coactivator for the ETS domain transcription factor PEA3. *Mol Cell Biol* 2006; **26**: 4529 - 4538.
28 Eo J, Han K, K MM, Song H, Lim HJ. Etv5, an ETS transcription factor, is expressed in granulosa and cumulus cells and serves as a transcriptional regulator of the cyclooxygenase-2. *J Endocrinol* 2008; **198**: 281 - 290.
29 Prat J. Prognostic parameters of endometrial carcinoma. *Human Pathol* 2004; **35**: 649 - 662.
30 Cavallaro U, Christofori G. Cell adhesion and signalling by cadherins and Ig-CAMs in cancer. *Nat Rev Cancer* 2004; **4**: 118 - 132.
31 Hurt EM, Saykally JN, Anose BM, Kalli KR, Sanders MM. Expression of the ZEB1 (deltaEF1) transcription factor in human: additional insights. *Mol Cell Biochem* 2008; **318**: 89 - 99.
32 Castilla MA, Moreno-Bueno G, Romero-Perez L, Van De Vijver K, Biscuola M, Lopez-Garcia MA *et al.* Micro-RNA signature of the epithelial-mesenchymal transition in endometrial carcinosarcoma. *J Pathol* 2011; **223**: 72 - 80.
33 Thiery JP, Acloque H, Huang RY, Nieto MA. Epithelial-mesenchymal transitions in development and disease. *Cell* 2009; **139**: 871 - 890.
34 Hanahan D, Weinberg RA. Hallmarks of cancer: the next generation. *Cell* 2011; **144**: 646 - 674.
35 Llaurado M, Abal M, Castellvi J, Cabrera S, Gil-Moreno A, Perez-Benavente A *et al.* ETV5 transcription factor is overexpressed in ovarian cancer and regulates cell adhesion in ovarian cancer cells. *Int J Cancer* 2011. e-pub ahead of print 25 April 2011; doi:10.1002/ijc.26148.
36 Petit MM, Fradelizi J, Golsteyn RM, Ayoubi TA, Menichi B, Louvard D *et al.* LPP, an actin cytoskeleton protein related to zyxin, harbors a nuclear export signal and transcriptional activation capacity. *Mol Biol Cell* 2000; **11**: 117 - 129.
37 Petit MM, Meulemans SM, Van de Ven WJ. The focal adhesion and nuclear targeting capacity of the LIM-containing lipoma-preferred partner (LPP) protein. *J Biol Chem* 2003; **278**: 2157 - 2168.
38 Swart GW, Lunter PC, Kilsdonk JW, Kempen LC. Activated leukocyte cell adhesion molecule (ALCAM/CD166): signaling at the divide of melanoma cell clustering and cell migration? *Cancer Metastasis Rev* 2005; **24**: 223 - 236.
39 Tavora B, Batista S, Reynolds LE, Jadeja S, Robinson S, Kostourou V *et al.* Endothelial FAK is required for tumour angiogenesis. *EMBO Mol Med* 2010; **2**: 516 - 528.
40 Chacon MR, Fazzari P. FAK: dynamic integration of guidance signals at the growth cone. *Cell Adh Migr* 2011; **5**: 52 - 55.
41 Monge M, Doll A, Colas E, Gil-Moreno A, Castellvi J, Garcia A *et al.* Subtractive proteomic approach to the endometrial carcinoma invasion front. *J Proteome Res* 2009; **8**: 4676 - 4684.
42 Irizarry RA, Hobbs B, Collin F, Beazer-Barclay YD, Antonellis KJ, Scherf U *et al.* Exploration, normalization, and summaries of high density oligonucleotide array probe level data. *Biostatistics* 2003; **4**: 249 - 264.
43 Smyth GK. Linear models and empirical bayes methods for assessing differential expression in microarray experiments. *Stat Appl Genet Mol Biol* 2004; **3**: Article 3.

Supplementary Information accompanies the paper on the Oncogene website (http://www.nature.com/onc)